Nanomed. J., 2(3): 223-230, Summer 2015
DOI: 10.7508/nmj. 2015.03.008

Simultaneous diagnosis and drug delivery by silymarin-loaded magnetic nanoparticles

[1]M. Khalkhali; [2]S. Sadighian; [3,4]K. Rostamizadeh; [1]F. Khoeini; [5]M. Naghibi; [2]N. Bayat; [3]M. Hamidi*

[1]*Department of Physics, University of Zanjan, Zanjan, Iran*
[2]*Department of Pharmaceutical biomaterials, School of Pharmacy, Zanjan University of Medical Sciences, Zanjan Iran*
[3]*Zanjan Pharmaceutical Nanotechnology Research Center, Zanjan University of Medical Sciences, Zanjan, Iran*
[4]*Department of Medicinal Chemistry, School of Pharmacy, Zanjan University of Medical Sciences, Zanjan, Iran*
[5]*Shahid Beheshti University of Medical Sciences, Tehran, Iran*

Received; 26 March 2015 Accepted; 15 June 2015

ABSTRACT:

Objective(s): The aim of this work was to prepare and characterize magnetic nanoparticles (MNPs) as theranostic system to act simultaneously as drug carrier and MRI contrast agent. Chitosan-coated MNPs (CMNPs) were prepared and loaded with silymarin. Silymarin-loaded CMNPs were characterized with various techniques and their potential as MRI contrast agent was also evaluated.

Materials and Methods: The chitosan-coated MNPs were prepared by coprecipitation method and were loaded with silymarin. The synthesized nanoparticles were characterized by various techniques including SEM, TEM, X ray diffraction (XRD), FTIR and vibrating sample magnetometer (VSM). In vitro drug release of silymarin was evaluated at 37 ÚC at pH 5.3 and 7.4. Then, their proton relaxivity was evaluated to study the potential of CMNPs as MRI contrast agent in terms of r_1 and r_2.

Results: Silymarin-loaded CMNPs were successfully prepared and characterized by FTIR and XRD techniques. VSM analysis revealed superparamagnetic properties of CMNPs. The release study showed that the maximum drug release accessible for CMNPs in pH=5.3 was higher than pH=7.4. Finally, the r_2/r_1 value of CMNPs was found to be close to 20 indicating that CMNPs has a strong efficiency as T_2 contrast agents for MRI imaging.

Conclusion: The findings demonstrated the potential of CMNPs as efficient MRI contrast agent as well as silymarin drug delivery.

Keywords: *Chitosan, Drug delivery systems, Magnetite, MRI contrast agent, Silymarin*

INTRODUCTION

Magnetic nanoparticles (MNPs) because of their unique properties such as small size, super-paramagnetism, low toxicity, etc, has found many applications in biomedicine for disease diagnosis and cancer therapy (e.g. MRI, drug delivery systems (DDS), hyperthermia) [1, 2]. To get benefit of MNPs in biomedicine, they should be stable for long term in aqueous solution, have particle size of less than 100 nm, and possess high magnetization. In addition, MNPs have to be coated in order to prevent the agglomeration and provide uniform distribution in suspension. There are different methods for preparation of stable dispersion of iron oxide in organic solvents including hexane and decane [3, 4]. In fact, for biological applications, it is vital to have stable MNPs in aqueous solution. So, to increase the stability of MNPs in aqueous solution, it is of great importance to use stabilizers such as surfactants, oxide or polymer compounds (especially bio-compatible polymer) with some specific functional groups on the surface of MNPs. In addition, the shell on the magnetic core provides a lot of significant advantages. It helps to

*Corresponding Author Email: *rostamizadeh@zums.ac.ir*
Tel: (+98) *241-34473635*

Note. This manuscript was submitted on March 26, 2015; approved on June 15, 2015

improve physical and chemical properties of the MNPs. It also has important role in protecting and stabilizing the core against the influence of acid, alkaline and oxidizing conditions, preparation of the nanoparticle with a desired surface charge and chemical functional group. Among different coatings, chitosan as a naturally drived polymer has been used extensively for modification of the surface MNPs owing to its biocompatibility and biodegra- dability [5]. Targeted therapy and controlled drug delivery are the principal aims of novel drug delivery systems. Carrier is the most important component of DDS, and it should be non toxic, should bind the drug properly, and make it possible to release intended drug at the target site. Currently, there are different kind of nanodrug delivery systems consisting of polymeric nano- particle, liposome, dan drimer and micelles [6]. Indeed, the role of nanoparticles (NP) is to improve their solubility, improve the therapeutic value of applied drugs by addition of retention time, and pass the biological barriers [7, 8, 9]. Nowadays, MNPs have attracted an immense deal of attention for drug delivery systems and MRI imaging [10,11]. Milk thistle (*Silybum marianum*, Asteraceae) seeds have been applied for centuries as treatment for several illnesses especially for liver. Silibinin, silychristin, and silidianin are the main component of milk thistle seed collectively known as silymarin extracted from milk thistle seeds, available commercially as standardized extract. Silymarin and its components (especially silibinin) have antioxidant, anti-inflammatory, immunomodulatory, lipid and biliary effects [12, 13]. Silibinin shows membrane protective confidants and it may protect blood constituents from oxidative damage [14, 15]. Silymarin shows low absorbtion and bioavability (between 20 and 50%), probably due to its degeneration by gastric fluid, poor enteral absorption or poor water solubility [16,17, 18]. Several methods including using a buccal liposomal delivery system [19], forming complexes with phospholipids [18] and incorporation into solid dispersions [20] have been reported to change the bioavailability of silymarin or silybin. Short half-life, low bioavailability and hydrophobic nature make it an appropriate candidate for gastrore-tentive drug delivery system. The MNPs can be used as drug carrier for drugs with lipophilic nature owing the advantage of being directed into the target tissue by its magnetic section. PLGA-PEG-MNPs is a kind of DDS have been reported where the pharmaceutical drugs was conjugated to the surface of PLGA-PEG-MNPs physically and released payload drug into the target site due to its external localized magnetic-field gradient [21, 22]. In the present contribution, chitosan-coated MNPs (CMNPs) were prepared and characterized as theranostic system to act simultaneously as drug carrier and MRI contrast agent. CMNPs were prepared and loaded with silymarin. Silymarin-loaded CMNPs were characterized with various techniques and their potential as MRI contrast agent was evaluated.

MATERIALS AND METHODS

Experimental

Silymarin was a gift from Barij Essence Pharmaceutical Company (Iran). Ferric chloride hexa-hydrate ($FeCl_3 \cdot 6H_2O$), ferrous chloride tetra-hydrate ($FeCl_2 \cdot 4H_2O$), NH_4OH (25% of ammonia), acetic acid (75%) and all solvents were from Merck and purchased locally. Chitosan was provided from Sigma. All the materials were used without any purification.

Preparation of iron oxide nanoparticles (MNPs)

Briefly, 1.62 g of ferric chloride was dissolved in 60 ml distilled water (0.1 M) under nitrogen gas atomosphere [23]. Then, 0.6 g of ferrous chloride dissolved in 30 ml of distilled water (0.1M), was added and the solution mixed under nitrogen for 15 min. Then diluted solution of NH_3 was added dropwise to the solution of iron salts when the color of the solution immediately changed to dark black. The precipitate was separated with strong external magnet (1.2 T) and washed several times with distilled water to remove any ions.

Preparation of chitosan-coated MNPs (CMNPs)

First, 20 mg of high molecular weight chitosan dissolved in 1 M acetic acid solution with final volume of 100 ml. Then 70 mg of MNPs were added to the solution and the mixture was mixed for 18 h.During this process, chitosan molecules were adsorbed on the surface of the MNPs and a dark brown suspension was obtained.

Preparation of silymarin-loaded CMNPs

Briefly, 50 mg CMNPs was added into 10 mg of silymarin (preliminarily solubilized in 5 ml ethanol) and stirred for 20 h. The silymarin-loaded CMNPs were separated by centrifugation at 14000 rpm and then washed three times with deionized water. The silymarin-

entrapped nanoparticles were dried in vacuumed oven at 30 ºC for 12 h. The unloaded silymarin was determined by measuring the concentration of drug in supernatant of centrifugation by UV-Vis spectrophotometry at wavelength of 288 nm. The entrapment efficiency was calculated using the following equation:

Entapment Efficiency (%) =(Total amount of drug-free amount of drug) / Total amount of drug (1)

Drug release study

The drug release behavior of nanoparticles were studied in physiological pH of 7.4 and acidic media with the pH of 5.3 in phosphate-buffered saline, PBS containing 0.5% (w/v) Tween 80. Typically, 10 mg of nanoparticles were placed into a dialysis bag (cut off 12 kDa) and introduced to 15 mL of PBS with desired pH under stirring (100 rpm) at 37 °C. At predetermined time intervals, in order to determine the drug concentration in dialysate and thereby time-dependent drug release profile, 1.0 mL of dialysate was taken out and replaced with 1.0 mL of fresh buffer solution maintained at 37 °C and assayed by UV–Vis spectroscopy at wavelength of 288 nm.

Characterization techniques

FT-IR spectra of nanoparticles were taken with a Bruker FT–IR spectrophotometer in the range of 400–4000 cm^{-1} as KBr disks. The morphology of the chitosan-coated MNPs was studied by field-emission scanning electron microscopy (FESEM, Mira 3-XMU). The magnetic properties of MNPs and the chitosan-coated MNPs were measured in vibrating sample magnetometer (VSM, LakeShore 7400) with an applied field between -20 to 20 kOe at 25 ÚC. The particle size distribution of the prepared CMNPs was determined by dynamic light scattering (DLS) (Malvern Instruments, UK, model Nano ZS).The structure and crystal phase of the CMNPs were measured by a Bruker D8 X-ray diffractometer with monochromated high-intensity Cu Ka radiation (k = 1.5418 Å) operated at 40 kV and 30 mA.

Magnetic resonance imaging (MRI) measurements

For measuring the magnetic relaxation property of the synthesized materials, MR imaging of CMNPs solutions with different iron concentrations of 0, 25, 50, 75, 100 and 200 µM were performed by using a clinical 1.5 T whole body magnetic resonance (MR) scanner (Siemens Healthcare Avanto Germany) at 25æ%C. T_1 images were measured with applying the spin echo imaging sequence at various repetition times of 100, 1550, 3150, 4750 and 6400 ms with an echo time of 18 ms, slice thickness: 7.5 mm, field of view (FOV): 230, and matrix: 200×256. The T2 images were obtained by using in the spin echo sequence with repetition times (TR) of 1600 ms and varying echo time (TE) of 10, 43, 75, 108 and 140 ms , slice thickness: 7.5 mm, field of view (FOV): 238, Turbo factor: 18, matrix: 176×384.Signal intensity with respect to each concentration was extracted from the resulting MRI images and Dicom Works 1.3.5 software and used to determine signal intensities within a manually drawn region of interest (ROI) for each sample. The signal intensity vs. TR or TE functions was exponentially fitted to the following equations(24, 25).

$$I = M_0[1 - \exp\left(-\frac{TR}{T_1}\right)] \quad (2)$$

$$I = M_0 \exp\left(-\frac{TE}{T_2}\right) \quad (3)$$

where I is the signal intensity and M_0 is constants. The longitudinal relaxivity r_1 and transverse relaxivity r_2, which represent the performance of the chitosan-coated MNPs as contrast agents, are calculated from the slope of the linear relationships.

RESULTS AND DISCUSSION

CMNPs with high dispersion capacity in aqueous solution provide stable ferrofluids which can be used for various biomedical applications (i.e. drug delivery systems and diagnostics). Moreover, the nanocarrier composed of magnetite nanoparticles can direct the payload drug toward the tumor sites with the support of an external magnetic field. On the other hand, because of the drug encapsulation via electrostatic bonding, they possess the capability to release the drug in the low-physiologic pH environments (pH 5–5.5), thereby targeting the lower-than-normal pH of the tumor sites as well as the media present in the endosomes of the cancer cells. The FT-IR spectra of CMNPs, silymarin and silymarin-loaded CMNPs are shown in Fig. 1. As shown in Fig 1a, the spectrum of CMNPs exhibited the absorption peaks at 1648, and 3274 cm^{-1} which can be attributed to N-H bending vibration and stretching vibration of amine functional group of chitosan, respectively. A strong absorption band at 557 cm^{-1} is characteristic peak of Fe-O band. Considering the chemical structure of chitosan and MNPs, hydroxyl and amino groups of chitosan form strong interaction with the surfaces of MNPs [27]. Fig 1b displays spectrum of

silymarin, peak at 1642 cm^{-1} is related to stretch vibration of -C=C- alkenes and absorption band at 1462 cm^{-1} is attributed to stretching vibration of C-C bands of aromatic groups. Fig 1c displays silymarin-loaded CMNPs. Apparently, the peak at 1642 cm^{-1} was shifted to 1591 cm^{-1}, and the peak at 557 cm^{-1} shifted to 569 cm^{-1} persumably due to the association between silymarin and CMNPs. Clearly, main absorption peaks of silymarin and chitosan-coated MNPs were appeared in the spectrum silymarin-loaded CMNPs indicating the successful silymarin payload into CMNPs.Fig 2 shows the crystalline structure of MNPs. Seven diffraction peaks (2q (111), (220), (311), (400), (422), (511) and (440)) were identified in XRD pattern demonstrating the inverse spinel structure of MNPs. After coating chitosan on MNPs, no significant change was observed. Using Debye Scherer's formula, the average nanoparticle size was calculated for uncoated and chitosan-coated MNPs to be 10.48 and 8.25 nm, respectively. The results show that the aggregation degree of the CMNPs is smaller than that of the naked MNPs.VSM graphs of MNPs and CMNPs are displayed in Fig. 3. Clearly, both of MNPs and CMNPs show superparamagnetic behaviors. As it is clear, the saturation magnetization of CMNPs was slightly lesser than that of MNPs. The reason behind this observation can be explained by the presence of chitosan on the surface of MNPs. Generally, it can be concluded that CMNPs has adequate superparamagnetic properties and could respond well to magnetic fields as a magnetic drug carrier for targeted delivery and MRI imaging.

Size and zeta potential measurements

The size of nanoparticles was analyzed by DLS technique. Particle size distribution curves showed only one peak with a relatively low polydispersity index. DLS histograms (Fig. 4 A and B) showed the particle size of MNPs and CMNPs to be 126 nm and 32 nm, respectively. The shape and morphology of nanoparticles were shown in Fig. 4 C-E. According to the Fig. 4C, the MNPs are in semi-spherical shape with mean size of 55 nm. Fig. 4D displays CMNPs in the same shape of the naked MNPs (4C), except the size of CMNPs which decreased to 18 nm. Fig. 4E shows TEM image of CMNPs with the average size of 12 nm. Indeed, different size obtained with DLS technique and SEM image can be explained by the fact that in spite of SEM image, DLS results imply to the hydrodynamic diameter of nanoparticles, while SEM results correspond to the particle size in dry condition. The zeta potentials of the naked MNPs in aqueous dispersion were determined to be -24.2 mV. Following coating MNPs with chitosan, zeta potential increased to + 31.6 mV demonstrating the presence of plentiful amino group of chitosan on the surface of targeting carrier (Fig 4F and G).

Drug loading and "In vitro" drug release studies

The results revealed that the drug loading and encapsulation efficiency for CMNPs were 10% and 95%, respectively. Fig 5 illustrates the drug release response of the CMNPs in PBS (0.1% Tween 80) with two different pH values of 5.3 and 7.4 at the physiological temperature of 37 °C. Clearly, there was no high initial burst release probably due to hydrophobic nature of silymarin. As it can be seen, silymarin-loaded CMNPs exhibited a sustained drug release over six days at pH 5.3 with the maximum attainable drug release close to 85 %. Controlled drug release characteristic of CMNPs verify the capability of these nanoparticles to be used as an impressive carrier in silymarin delivery system.

MRI contrast enhancement

The longitudinal (T_1) and transverse (T_2) relaxation times were measured at various solutions of different iron concentrations using a clinical 1.5 T whole body magnetic resonance (MR) scanner. Fig. 6 shows T_1-weighted MR images of chitosan-coated MNPs with iron concentrations of 0, 25, 50, 75, 100 and 200 µM in deionized water. It illustrates a dose dependent signal change which is due to the relaxation increase of the water proton with increasing the dose. The magnetic susceptibility of the iron oxide nanoparticles produce local field gradients that accelerates the dephasing of the spins of the surrounding water molecules and

Table 1. The longitudinal relaxivity (r_1, $mM^{-1}s^{-1}$), transverse relaxivity (r_2, $mM^{-1}s^{-1}$), r_2/r_1 values and R^2 of chitosan-coated magnetite nanoparticles was calculated by plotting the T_1 relaxation rate ($1/T_1$) and T_2 relaxationrate ($1/T_2$) as a function of Fe concentration

nanoparticles	r_1 ($mM^{-1}s^{-1}$)	R^2	r_2 ($mM^{-1}s^{-1}$)	R^2	r_2/r_1
chitosan coated MNPs	4.708	0.799	91.44	0.943	19.42

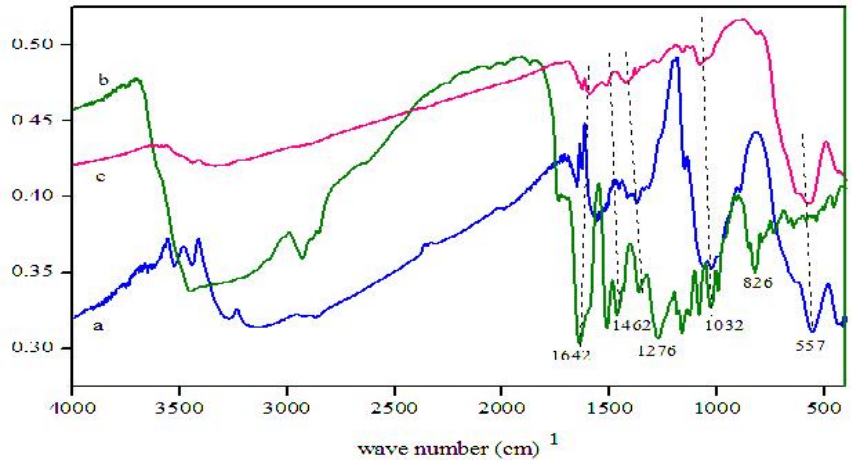

Fig. 1. FT-IR spectra of (a) CMNPs (b) silymarin (c) silymarin loaded CMNPs

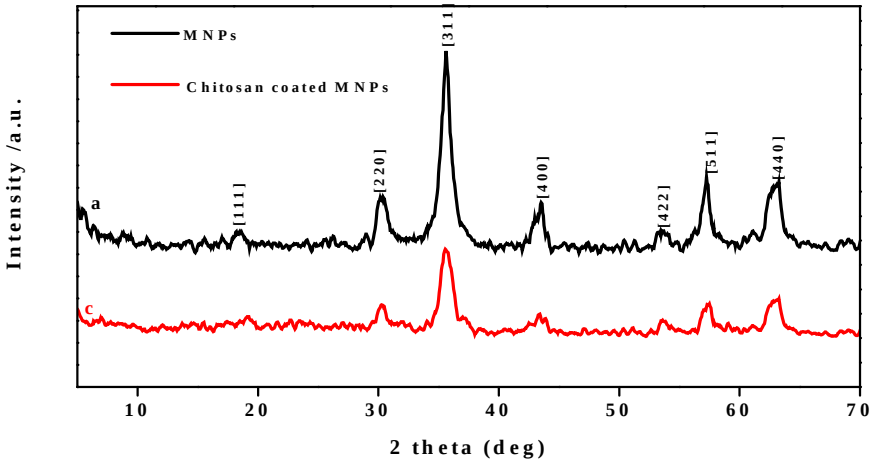

Fig. 2. XRD pattern of (a) MNPs and (b) CMNPs

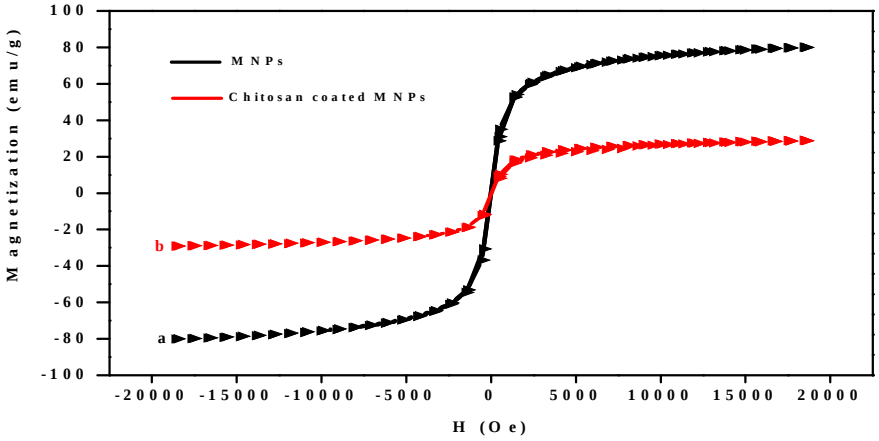

Fig. 3. VSM curves of (a) MNPs and (b) CMNPs

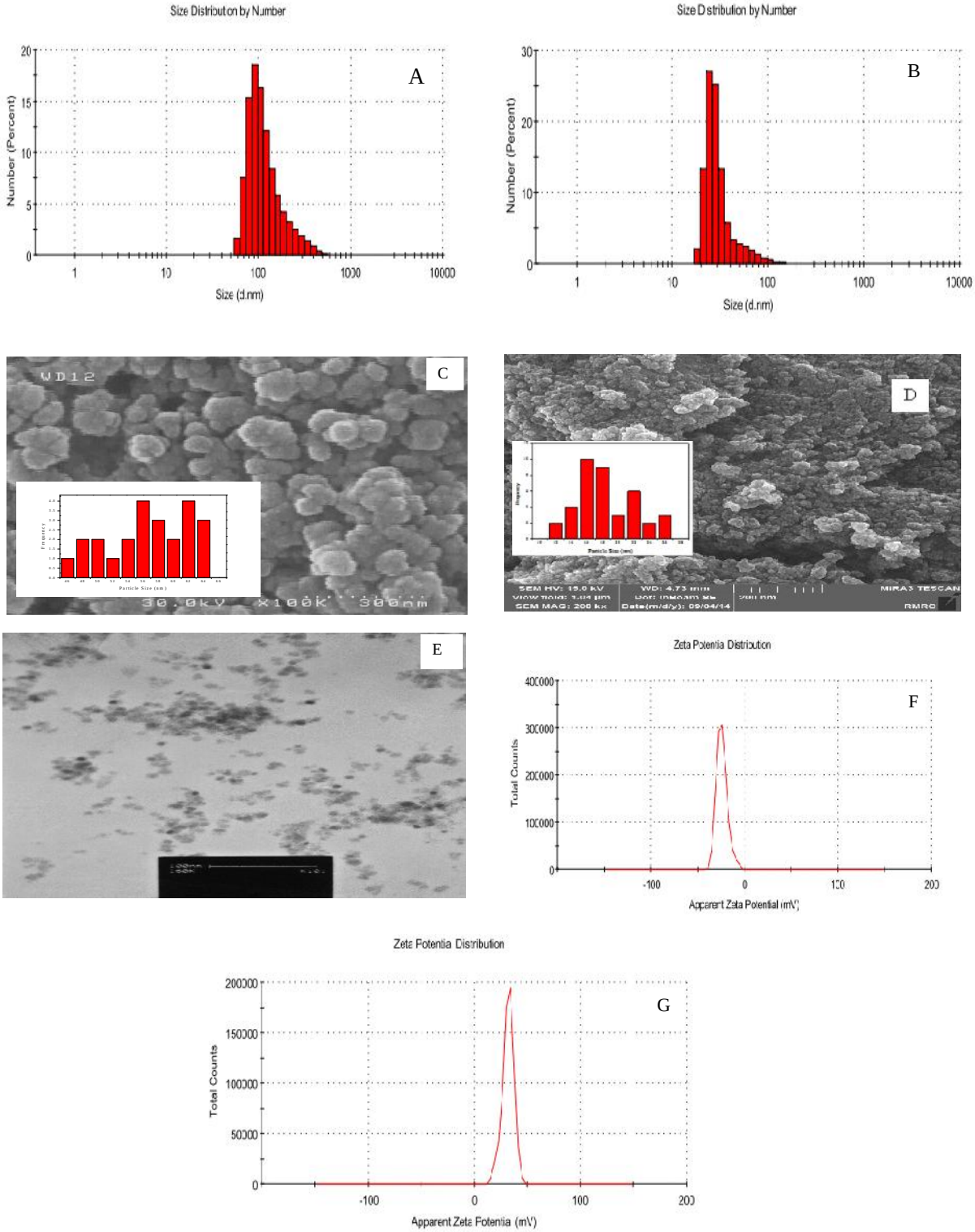

Fig. 4. Size distribution of (A) MNPs (B) CMNPs assessed by DLS, (C) FESEM image of MNPs, (D) CMNPs, (E) TEM image of CMNPs, and (F) zeta potential of MNPs (G) and CMNPs (F)

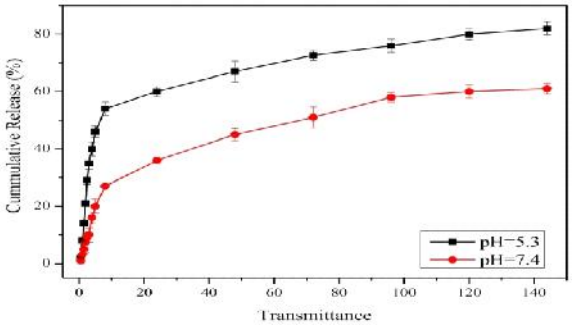

Fig. 5. In vitro drug release profile of silymarin from CMNPs at pH= 5.3 and 7.4

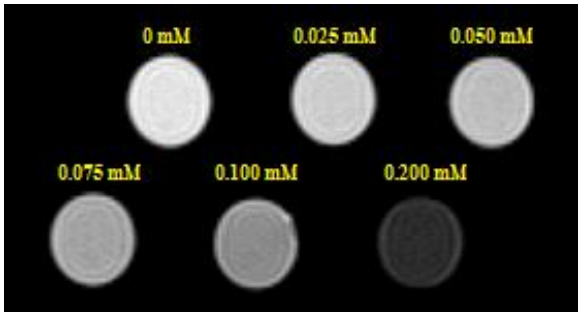

Fig .7. T_2-weighted MRI images (1.5T, spin-echo sequence: repitition time TR = 1600 ms, echo time TE = 108 ms) of the CMNPs at various iron concentration at 25°C

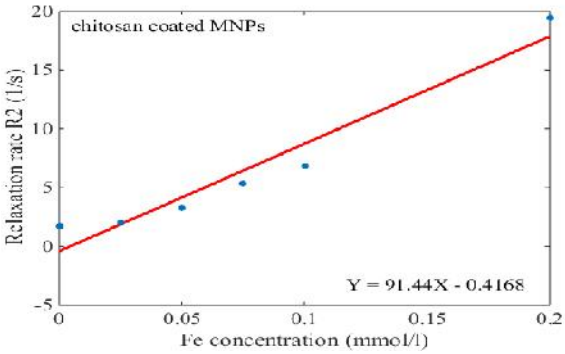

Fig. 9. T_2 relaxation rate plotted as a function of Fe concentration (mM) for CMNPs

raises spin–spin relaxation time (T_2). Fig. 7 shows T_2-weighted MR images of CMNPs with different iron concentration and illustrates a signal drop of the phantom images with increasing iron concentration. The r_1 and r_2 were calculated to be 4.708 and 91.44 $mM^{-1}s^{-1}$ from the slopes of the $1/T_1$ (R_1) and $1/T_2$ (R_2) plots versus Fe concentration, respectively (Fig. 7 and

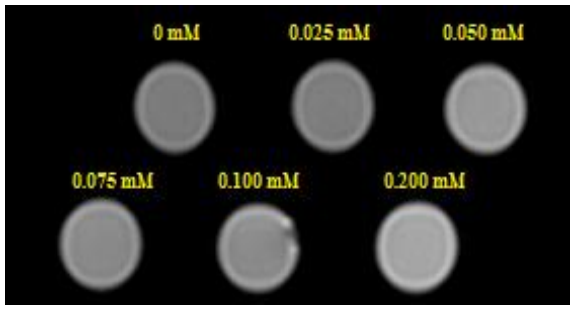

Fig . 6. T_1-weighted MRI images (1.5T, spin-echo sequence: repitition time TR = 1550 ms, echo time TE = 18 ms) of the CMNPs at various iron concentration at 25°C

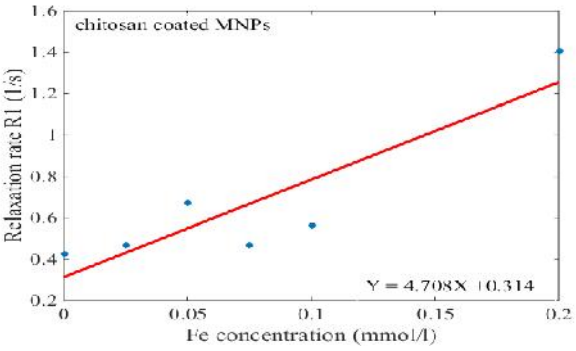

Fig. 8. T_1 relaxation rate plotted as a function of Fe concentration (mM) for CMNPs

Fig. 8). The calculated r_1, r_2 and r_2/r_1 values are shown in Table 1. It has been reported that magnetic nanoparticles are commonly used as T_2 MRI contrast agents and consequently they are able to decrease the MR signal intensity [28]. The efficiency of a contrast agent is determined by ratio between transverse and longitudinal relaxivity (r_2/r_1). The r_2/r_1 ratio for CMNPs was determined to be 19.42 which is higher than that of Resovist, commercially available MRI contrast agent [29]. This finding indicates that CMNPs could be considered as promising T2 contrast agent with strong T_2 shortening effect.

CONCLUSIONS

In the present study, a novel CMNPs was synthesized by co-precipitation method. Chitosan was selected to provide steric stabilization around MNPs and provide stable aqueous dispersion. The FT-IR confirmed the successful synthesis of CMNPs. Particle size analysis (DLS) and scanning electron microscopy (SEM) confirmed the formation of spherical nanoparticles with the final

average particle size about 18 nm. The VSM analysis demonstrated the saturation magnetization values of 29.08 emu/g for CMNPs. Entrapment efficiency and drug loading for silymarin were calculated to be 95 and 10%, respectively. The finding revealed that CMNPs provide a sustained release pattern. It was found that the maximum drug release accessible for CMNPs in pH=5.3 was higher than pH=7.4. The the r_2/r_1 value of CMNPs was determined to be 19.42 indicating that the developed formulation has a strong efficiency as T_2contrast agents and controlled silymarin delivery.

ACKNOWLEDGMENT

We are most grateful for the continuing ûnancial support of this research project by Zanjan University of Medical Sciences and University of Zanjan.

REFERENCES

1. Pankhurst QA, Connolly J, Jones S, Dobson J. Applications of magnetic nanoparticles in biomedicine. J Phys D: Appl Phys. 2003; 36(13): R167.
2. Gupta AK, Gupta M. Synthesis and surface engineering of iron oxide nanoparticles for biomedical applications. Biomaterials. 2005; 26(18): 3995-4021.
3. Shafi KV, Ulman A, Yan X, Yang N-L, Estournes C, White H, et al. Sonochemical synthesis of functionalized amorphous iron oxide nanoparticles. Langmuir. 2001; 17(16): 5093-7.
4. Fried T, Shemer G, Markovich G. Ordered Two Dimensional Arrays of Ferrite Nanoparticles. Adv Mater. 2001; 13(15): 1158-61.
5. Mai TTT, Ha PT, Pham HN, Le TTH, Pham HL, Phan TBH, et al. Chitosan and O-carboxymethyl chitosan modified Fe_3O_4 for hyperthermic treatment. Adv Nat Sci: Nanosci Nanotechnol. 2012; 3(1): 015006.
6. Ali I, Salim K, A Rather M, A Wani W, Haque A. Advances in nano drugs for cancer chemotherapy. Current cancer drug targets. 2011; 11(2): 135-46.
7. Shenoy DB, Amiji MM. Poly (ethylene oxide)-modified poly ([-caprolactone) nanoparticles for targeted delivery of tamoxifen in breast cancer. Int J Pharm. 2005; 293(1): 261-70.
8. Safra T, Muggia F, Jeffers S, Tsao-Wei D, Groshen S, Lyass O, et al. Pegylated liposomal doxorubicin (doxil): reduced clinical cardiotoxicity in patients reaching or exceeding cumulative doses of 500 mg/m2. Ann Oncol. 2000; 11(8): 1029-33.
9. Alexis F, Pridgen E, Molnar LK, Farokhzad OC. Factors affecting the clearance and biodistribution of polymeric nanoparticles. Mol Pharm. 2008; 5(4): 505-15.
10. Grassi-Schultheiss P, Heller F, Dobson J. Analysis of magnetic material in the human heart, spleen and liver. Biometals. 1997; 10(4): 351-5.
11. Hu F, Neoh K, Kang E. Synthesis and in vitro anti-cancer evaluation of tamoxifen-loaded magnetite/PLLA composite nanoparticles. Biomaterials. 2006; 27(33): 5725-33.
12. DerMarderosian A, Beutler JA. The review of natural products: the most complete source of natural product information: Facts and Comparisons; 2002.
13. Evans W. Trease and Evans pharmacognosy (2002). WB Saunders, China.193-407.
14. Das SK, Mukherjee S, Vasudevan D. Medicinal properties of milk thistle with special reference to silymarin: An overview. Nat Prod Rad. 2008; 7: 182-92.
15. Kshirsagar A, Ingawale D, Ashok P, Vyawahare N. Silymarin: a comprehensive review. Pharmacogn Rev. 2009;3(5):116-24.
16. Blumenthal M, Goldberg A, Brinckmann J. Herbal Medicine. Expanded Commission E monographs: Integrative Medicine Communications; 2000.
17. Comoglio A, Tomasi A, Malandrino S, Poli G, Albano E. Scavenging effect of silipide, a new silybin-phospholipid complex, on ethanol-derived free radicals. Biochem Pharmacol. 1995; 50(8): 1313-6.
18. Giacomelli S, Gallo D, Apollonio P, Ferlini C, Distefano M, Morazzoni P, et al. Silybin and its bioavailable phospholipid complex (IdB 1016) potentiate in vitro and in vivo the activity of cisplatin. Life Sci. 2002; 70(12): 1447-59.
19. El-Samaligy M, Afifi N, Mahmoud E. Increasing bioavailability of silymarin using a buccal liposomal delivery system: preparation and experimental design investigation. Int J Pharm. 2006; 308(1): 140-8.
20. Li F-Q, Hu J-H, Jiang Y-Y. Preparation and characterization of solid dispersions of silymarin with polyethylene glycol 6000. J. Chin. Pharm. Sci. 2003;12(2):76-81.
21. Yoo HS, Park TG. Biodegradable polymeric micelles composed of doxorubicin conjugated PLGA–PEG block copolymer. J Control Release. 2001; 70(1): 63-70.
22. Avgoustakis K, Beletsi A, Panagi Z, Klepetsanis P, Karydas A, Ithakissios D. PLGA–mPEG nanoparticles of cisplatin: in vitro nanoparticle degradation, in vitro drug release and in vivo drug residence in blood properties. J Control Release. 2002; 79(1): 123-35.
23. Mohammadi-Samani S, Miri R, Salampour M, Khalighian N, Sotoudeh S, Erfani N. Preparation and assessment of chitosan-coated superparamagnetic Fe_3O_4 nanoparticles for controlled delivery of methotrexate. Res Pharm Sci. 2013; 8(1): 25-33.
24. Arsalani N, Fattahi H, Nazarpoor M. Synthesis and characterization of PVP-functionalized superparamagnetic Fe_3O_4 nanoparticles as an MRI contrast agent. Express Polym Lett. 2010; 4(6): 329-38.
25. Lee N, Hyeon T. Designed synthesis of uniformly sized iron oxide nanoparticles for efficient magnetic resonance imaging contrast agents. Chem Soc Rev. 2012; 41(7): 2575-89.
26. Shrifian-Esfahni A, Salehi MT, Esfahani MN, Ekramian E. Chitosan-modified superparamgnetic iron oxide nanoparticles: design, fabrication, characterization and antibacterial activity. CHEMIK. 2015; 69(1): 19–32.
27. Qiang L, Li Z, Zhao T, Zhong S, Wang H, Cui X. Atomic-scale interactions of the interface between chitosan and Fe_3O_4. Colloids Surf A Physicochem Eng Asp. 2013; 419: 125-32.
28. Saraswathy A, Nazeer SS, Nimi N, Arumugam S, Shenoy SJ, Jayasree RS. Synthesis and characterization of dextran stabilized superparamagnetic iron oxide nanoparticles for in vivo MR imaging of liver fibrosis. Carbohydr Polym. 2014;101:760-8.
29. Ma X, Gong A, Chen B, Zheng J, Chen T, Shen Z, et al. Exploring a new SPION-based MRI contrast agent with excellent water-dispersibility, high specificity to cancer cells and strong MR imaging efficacy. Colloids Surf B Biointerfaces. 2015; 126: 44-9.

How to cite this article:
Khalkhali M, Sadighian S, Rostamizadeh K, Khoeini F, Naghibi M, bayat N, Hamidi M. Simultaneous diagnosis and drug delivery by silymarin-loaded magnetic nanoparticles. Nanomed. J., 2015; 2(3): 223-230.